

**CLEARINGHOUSE FOR FEDERAL SCIENTIFIC AND TECHNICAL INFORMATION CFSTI
DOCUMENT MANAGEMENT BRANCH 410.11**

LIMITATIONS IN REPRODUCTION QUALITY

ACCESSION # *AD 609 024*

- ☒ 1. WE REGRET THAT LEGIBILITY OF THIS DOCUMENT IS IN PART UNSATISFACTORY. REPRODUCTION HAS BEEN MADE FROM BEST AVAILABLE COPY.
- ☐ 2. PORTION OF THE ORIGINAL DOCUMENT CONTAINS FINE DETAIL WHICH MAY MAKE READING OF PHOTOCOPY DIFFICULT.
- ☐ 3. THE ORIGINAL DOCUMENT CONTAINS COLOR, BUT DISTRIBUTION COPIES ARE AVAILABLE IN BLACK-AND-WHITE REPRODUCTION ONLY.
- ☐ 4. THE INITIAL DISTRIBUTION COPIES CONTAIN COLOR WHICH WILL BE SHOWN IN BLACK-AND-WHITE WHEN IT IS NECESSARY TO REPRINT.
- ☐ 5. LIMITED SUPPLY ON HAND: WHEN EXHAUSTED, DOCUMENT WILL BE AVAILABLE IN MICROFICHE ONLY.
- ☐ 6. LIMITED SUPPLY ON HAND: WHEN EXHAUSTED DOCUMENT WILL NOT BE AVAILABLE.
- ☐ 7. DOCUMENT IS AVAILABLE IN MICROFICHE ONLY.
- ☐ 8. DOCUMENT AVAILABLE ON LOAN FROM CFSTI (TT DOCUMENTS ONLY).
- ☐ 9.

PROCESSOR:

TSL-107-10/64

V. Ritenour

Penetration and Cratering Study
Air Force Ballistic Missiles Division
Contract No. AF 04(647)-176

40

13 NA

14 Incl.

6

PENETRATION AND PERFORATION STUDIES

OF

THIN GLASS TARGETS

by

7 NA

8 Merlin D. Fullmer, Wm. S. Partridge,
and Emerson T. Cannon

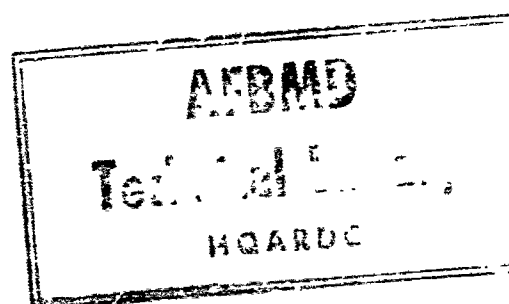
9

Technical Report UU-2

10 Iv. incl.
in. table

9

August 1958



ABSTRACT

Steel spheres $3/32$ inches in diameter were accelerated to velocities in the range of 0.1 to 2.5 km/sec. and impacted normally upon ordinary plate glass targets 4 inches square and $3/64$, $1/16$, $1/8$, $1/4$ and $1/2$ inches thick. Tungsten spheres $1/16$ inches in diameter were also impacted in the same manner as the steel spheres at velocities from 2.0 to 2.5 km/sec. into $1/4$ - and $1/2$ -inch thick glass. Steel BB shot $1/4$ inch in diameter were impacted in the same manner as previously described into the $3/64$ -inch thickness at the 0.1 km/sec. velocity range.

It was found that the kinetic energy lost by the pellet during perforation of the target was a function of the impact velocity to the second power. Therefore, parabolas could be used to approximate these curves.

The plot of the minimum velocity of perforation as a function of target thickness was found to be a straight line relationship.

The manner in which the energy dissipates in the glass was qualitatively explained.

TABLE OF CONTENTS

| | <u>Page</u> |
|-----------------------------------|-------------|
| INTRODUCTION | 1 |
| EXPERIMENTAL TECHNIQUES | 4 |
| RESULTS | 9 |
| CONCLUSIONS | 31 |
| APPENDIX 1 | |
| APPENDIX 2 | |

INTRODUCTION

Horsley¹ used long-time-loading machines which applied the load in the form of a steel ball to the surface of a plate of glass. He found that the strength of all types of glass, up to the limits of his measurements, increased with the rate of loading. Rate of loading is defined as the increase of the load per unit time as applied to the surface of the glass.

Stanworth,² while corroborating the long-known fact that glass fracture occurs perpendicular to the tensile stress, also pointed out that the glass endured much higher stress when a small ball was pressed against the surface of a plate glass than when a large ball was used. The existing theory during stanworth's time, as expounded by Griffith,³ explained this fracture qualitatively but quantitatively could not predict the breaking stress with greater accuracy than a factor of 10 to 100.

According to the Griffith crack theory, the mechanism of fracture is regarded as follows: First, there is an elongation of the sample so that an element of length is increased by a small amount. This increase in length being distributed in a statistical way among many bonds, it is imagined that the small increase in length is then relatively suddenly concentrated in the bond producing fracture. The elongation supposedly

-
1. Horsley, "Static Fatigue Studies of Glass," Thesis, Dept. of Physics, University of Utah, Salt Lake City (1953).
 2. Stanworth, J. E., "Physical Properties of Glass," Clarendon Press (1950).
 3. Griffith, A. A., "Philosoph. Trans. Royal Soc.," 221-a, 182-183, 192 (1921).

takes place by slow orientation of atoms, involving an activation energy for each unit of elongation.

It was the work of Charles⁴ which hinted that the Griffith theory was inadequate. Charles used mild steel projectiles and impacted them at high velocities into small pyrex glass cylinders. His results indicated that the energy required to fracture a brittle object at high velocity impact was considerably less than that required to fracture the object at low velocity impact. Later work by Charles⁵ using a fixed-free glass rod which was struck with a hammer indicated that the transfer of the kinetic energy of impact to the rod was greatly dependent on the time during which the hammer and the rod remained in contact. He found that the maximum energy transfer occurred when the impact time was 0.8 of the natural frequency of vibration for the pyrex rod. Study of the rate of crack propagation by Kolsky⁶ combined with the investigation of glass structure through X-ray techniques by Grjotheim⁷ indicated that perhaps the Griffith theory, although useful for statistic and slow velocity impact tests, was quite inadequate for the purposes of rapid impact. Grjotheim's work proved conclusively that glass has an irregular, continuous molecular structure and is not formed of small crystals as might be inferred from the Griffith theory.

4. Charles, R. J., "High Velocity Impact in Comminution," Min. Eng. 8 (1956).

5. Ibid.

6. Kolsky, H., "Fracture and Cavitation in Glassy Materials," Clarendon Press, Oxford Press, Oxford (1953).

7. Grjotheim, K., "Use of X-ray Methods for Investigations of Glass Structure," Glass Industry, April, (1958).

It was Poncelet⁸ who, by the use of a Born system of forces and the individual particle theory, showed that the fracture of glass is a rate process.

Since the mechanism of glass fracture is a function of time, then we might expect the kinetic energy dissipated by the fracture of the glass to be a function of impact time. If small steel pellets were shot through thin glass targets, and the velocity of the pellet varied from that required to just perforate the glass to some considerably higher velocity approaching the crack propagation rate, the time dependence of the fracturing process should be observed in the form of kinetic energy the pellet lost compared with the impact velocity. It was the purpose of this report to discover the relationship between the kinetic energy the pellet lost during perforation of the target as a function of target thickness, and pellet impact velocity.

8. Poncelet, E. F., "Modern Concepts of Fracture and Flow," Glass Industry, 38, No. 10, Oct. (1957).

EXPERIMENTAL TECHNIQUES

Figure A shows the general arrangement of the equipment used. The pellet, usually a steel sphere of approximately $3/32$ inch diameter, was accelerated by a gun powder charge contained in a 220 Swift cartridge. A sabot⁹ held the pellet until they both left the gun, whereupon the sabot was stopped by the blast shield. The velocity of the pellet was controlled by varying the type and the amount of the gun powder contained in the cartridge.

Figure 1 shows the schematic arrangement of the equipment used in conducting this test. The "spider"¹⁰ placed approximately 900 volts across the Mylar¹¹ foils. This voltage caused a temporary arc to occur wherever the insulator of the Mylar was damaged. The arc burned the adjacent conducting material and thereby prevented another arc at this particular location of the foil. After all of the damaged sections of the foil had been effectively removed by arcing, the spider was turned off.

The velocity of the pellet was measured by two methods. The first method used employed two Berkeley counting units. The pulse formed by the arcing Mylar when the pellet passed through it started and then stopped the first counting unit as the pellet passed through the first and second foils, respectively. The time displayed by the counter was used to calculate the impact velocity. Perforation of the third and

9. Partridge, W. S., Vanfleet, H. B., and Whited, C. R., Technical Report No. OSR-9, Contract No. AF 18(600) 1217.

10. See Appendix 2.

11. Ibid.



Fig. A. Perspective of testing equipment

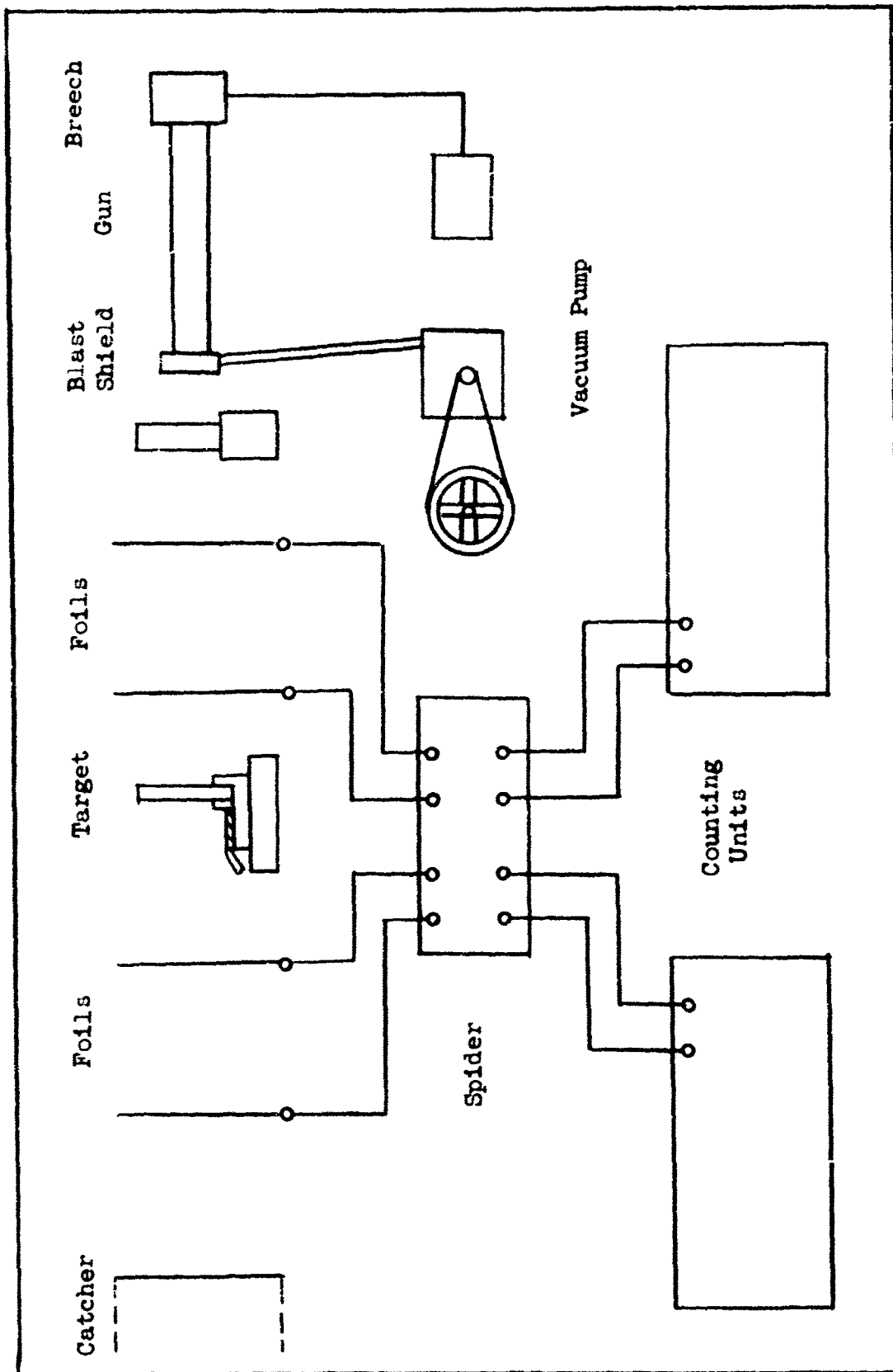


Fig. 1. Block diagram of test setup.

fourth foils resulted in a time display by the second counter. This interval was used to compute the exit velocity of the pellet.

The second method used to measure the velocity of the pellet employed a Tektronix two-channel oscilloscope. The pulse from the first foil started the horizontal trace on Channel A. The second pulse temporarily deflected the cathode ray beam vertically off scale. The second set of foils produced a similar trace through Channel B. The velocity was computed by examining the distance from the start of the trace to the break caused by the pellet. The distance was a known function of time as determined by the horizontal sweep setting. The information displayed by the oscilloscope was recorded by a Dumont Type 302 camera.

When the pellet perforated the timing foils, the target, or the second blast shield, it lost kinetic energy. Therefore, in order that only the kinetic energy lost during perforation of the target was measured, it was necessary to compensate for the energy lost to the shield and foils. It was found that for the velocity ranges considered, subtraction of 20 microseconds from the time indicated by the counting units corrected for the energy lost during perforation of the foils. This was shown by shooting through the foils with no target present and varying the velocity of the pellet from the minimum to the maximum as determined by the actual shots when targets were used. Subtraction of an additional 20 microseconds compensated for the energy loss incurred by perforation of the second blast shield, which was one sheet of paper from an "Efficiency" Legal Pad No. 364L. The purpose of the second blast shield was to stop the fractured pieces of glass from perforating the second set of timing foils. Perforation of the second set of timing foils by the glass, it was thought, would adversely affect the counting time.

The highest velocities were obtained by evacuation of the air in the barrel of the gun by using a Duo Seal vacuum pump.

RESULTS

A summary of kinetic energy lost during perforation as a function of the pellet impact velocity is given by the plots of Figs. 2 through 6, which correspond to the tabulation of Tables 1 through 5, respectively. The curves were assumed to be of the form $y = Ax^2$, where y was the kinetic energy in joules lost during perforation and x was the impact velocity in kilometers per second. A summary of Figs. 2 through 6 is given by Fig. 7. The calculated equations for the curves were as follows:

| <u>Thickness of Glass</u> <u>(inches)</u> | <u>Calculated Parabola</u> |
|--|----------------------------|
| 3/64 | $y = 9.20 x^2$ |
| 1/16 | $y = 13.75x^2$ |
| 1/8 | $y = 20.60x^2$ |
| 1/4 | $y = 16.5 x^2$ |
| 1/2 | $y = 18.7 x^2$ |

The best curve fit was obtained by eye. There was not any obvious relationship between the constant for the parabola and the thickness of the target.

The minimum energy of perforation as a function of target thickness is given by the plot of Fig. 8. Approximately five shots were used to determine the minimum energy of perforation for each target thickness.

The steel pellet was greatly deformed at the higher velocities and for the 1/2-inch and 1/4-inch targets. Tungsten pellets were shot through the 1/2-inch and 1/4-inch targets at the same velocities. The outside of the tungsten sphere tended to crumble. The kinetic energy

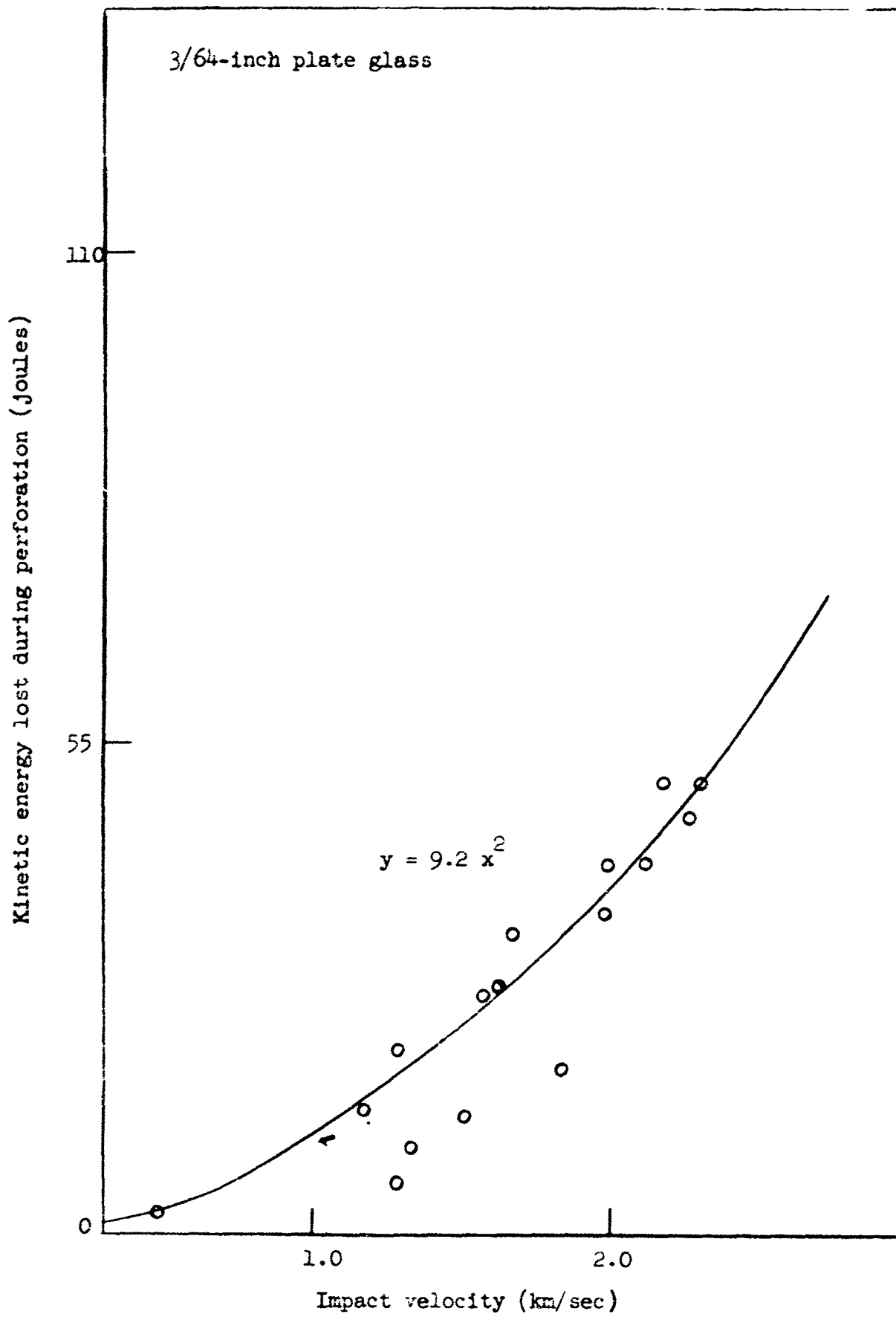


Fig. 2

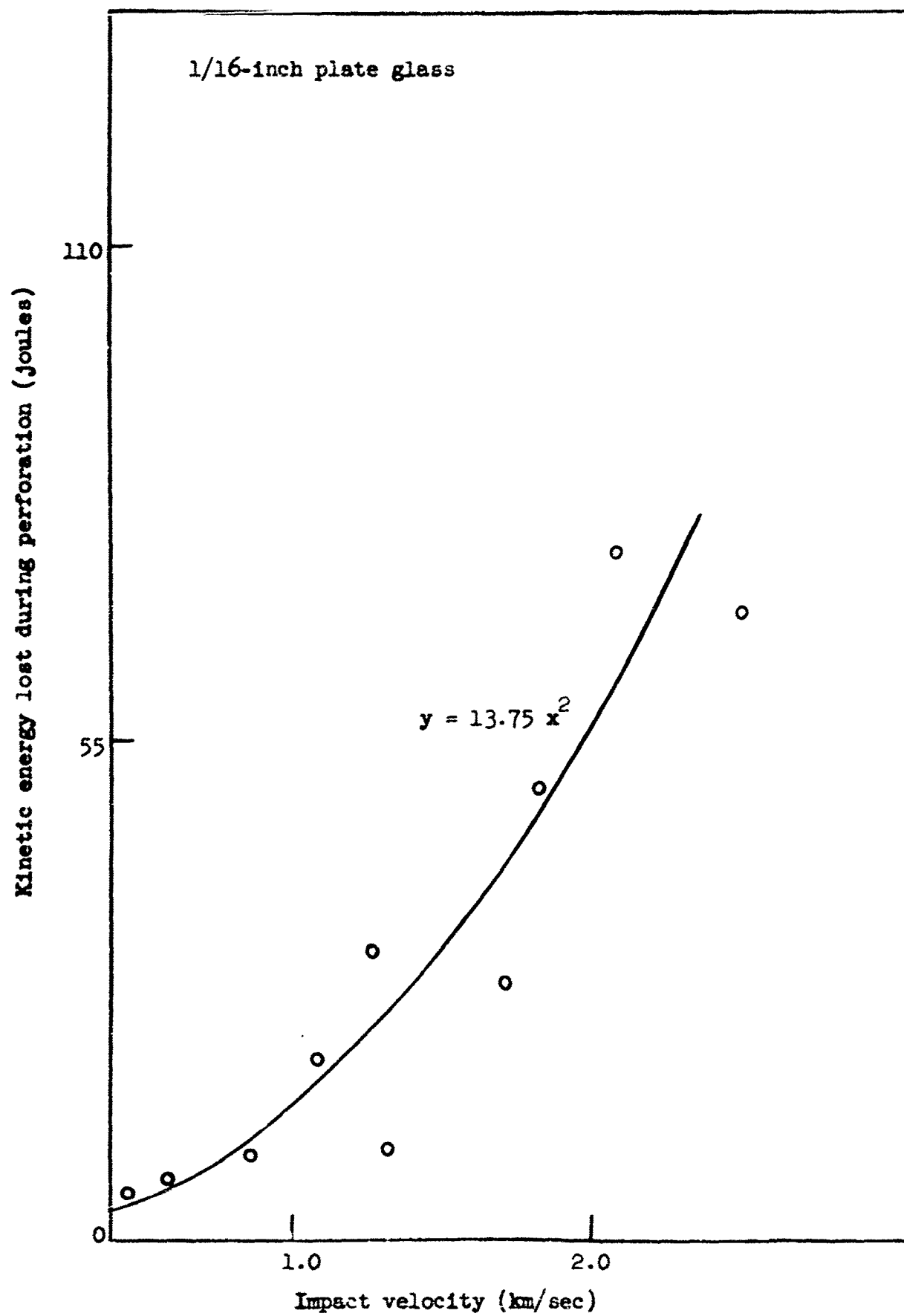


Fig. 3

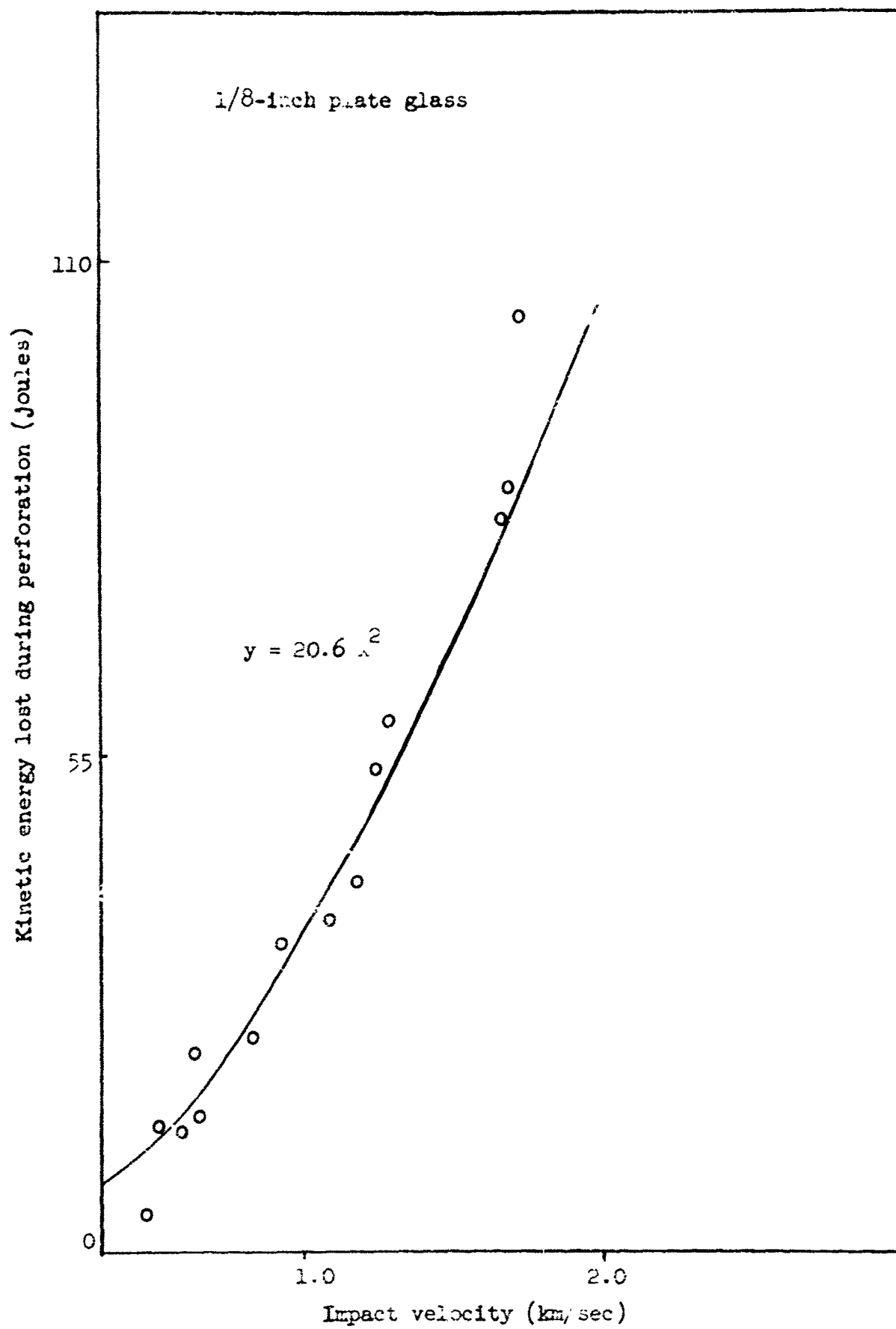


Fig. 4

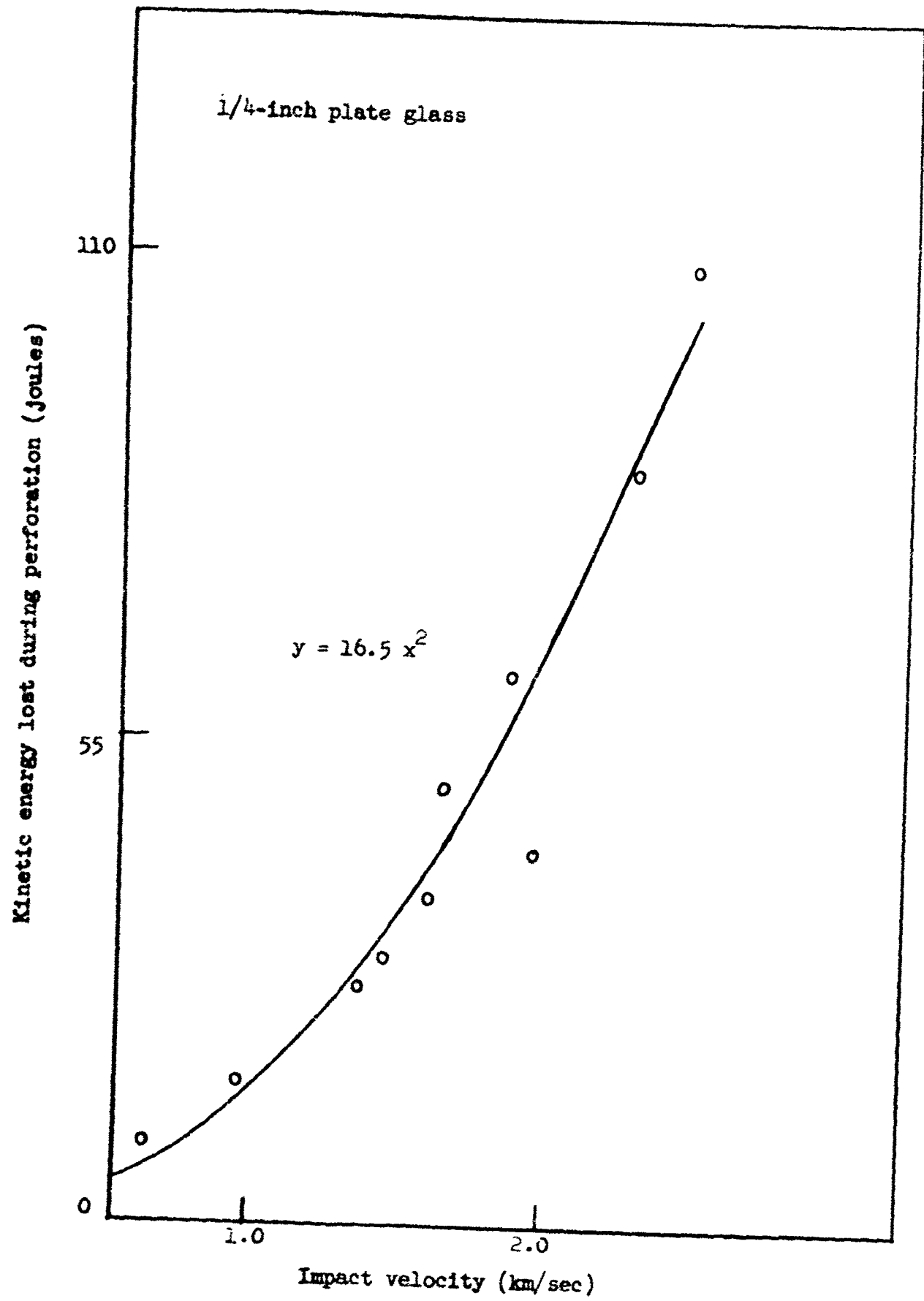


Fig. 5

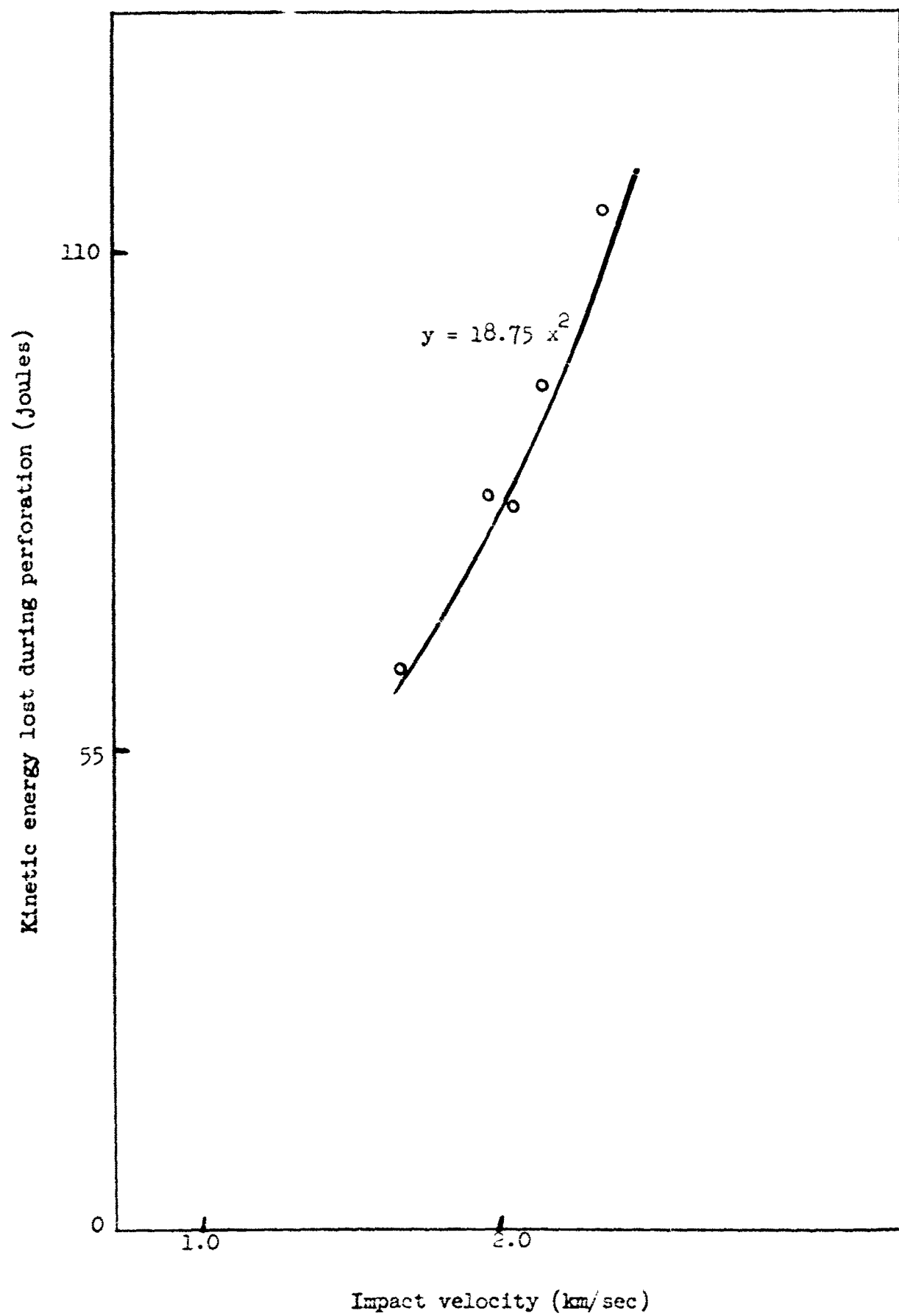


Fig. 6

TABLE 1

3/64-Inch Plate Glass

| Shot No. | V_{impact} (km/sec) | V_{exit} (km/sec) | V_{in}^2 | V_{ex}^2 | $V_{\text{in}}^2 - V_{\text{ex}}^2$ | K.E. (joules) |
|----------|---------------------------------|-------------------------------|-------------------|-------------------|-------------------------------------|---------------|
| 1 | 2.17 | 1.79 | 4.71 | 3.19 | 1.52 | 41.7 |
| 2 | 2.26 | 1.82 | 5.15 | 3.30 | 1.85 | 51.0 |
| 3 | 1.66 | 1.5 | 2.77 | 2.30 | 0.47 | 10.9 |
| 4 | 1.79 | 1.47 | 3.19 | 2.16 | 1.03 | 28.8 |
| 5 | 1.75 | 1.45 | 3.06 | 2.10 | 0.96 | 26.4 |
| 6 | 1.43 | 1.33 | 2.04 | 1.78 | 0.26 | 7.2 |
| 7 | 1.41 | 1.30 | 1.98 | 1.70 | 0.19 | 5.2 |
| 8 | 1.47 | 1.35 | 2.16 | 1.83 | 0.33 | 9.1 |
| 9 | 1.39 | 1.08 | 1.03 | 1.18 | 0.75 | 20.6 |
| 10 | 1.31 | 1.11 | 1.73 | 1.24 | 0.49 | 13.5 |
| 11 | 1.02 | --- | 1.04 | --- | 1.04 | 28.6 |
| 14 | 1.08 | --- | 1.18 | --- | 1.18 | 32.4 |
| 15 | 1.85 | 1.66 | 3.42 | 2.78 | 0.64 | 17.6 |
| 16 | 1.56 | 1.39 | 2.34 | 1.93 | 0.41 | 11.3 |
| 17 | 2.27 | 1.85 | 5.15 | 3.42 | 1.73 | 47.5 |
| 18 | 1.72 | 1.31 | 2.96 | 1.73 | 1.23 | 33.8 |
| 19 | 2.32 | 1.88 | 5.40 | 3.55 | 1.85 | 51.0 |
| 20 | 2.00 | 1.64 | 4.00 | 2.69 | 1.31 | 36.0 |
| 21 | 1.42 | 1.35 | 2.03 | 1.82 | 0.21 | 5.76 |
| 22 | 2.01 | 1.61 | 4.11 | 2.60 | 1.51 | 41.5 |
| 23 | 0.071 | 0.00 | 0.005 | --- | 0.035 | 0.95 |
| 24 | 0.086 | --- | 0.051 | --- | 0.051 | 1.40 |
| 25 | 0.102 | --- | 0.072 | --- | 0.072 | 1.97 |
| 26 | 0.068 | --- | 0.031 | --- | 0.031 | 0.87 |
| 27 | 0.048 | --- | 0.015 | --- | 0.015 | 0.04 |
| 28 | 0.057 | --- | 0.022 | --- | 0.022 | 0.06 |

Note: Shots 23 to 28 were taken using a steel BB 1/8" diameter, wt. 0.343 gm. All other shots for Table 1 were taken with 3/32" diameter steel sphere, wt. 0.052 gm.

TABLE 2

1/16-Inch Plate Glass

| Shot No. | V_{impact} (km/sec) | V_{exit} (km/sec) | V_{in}^2 | V_{ex}^2 | $V_{\text{in}}^2 - V_{\text{ex}}^2$ | K.E. (joules) |
|-------------|---------------------------------|-------------------------------|-------------------|-------------------|-------------------------------------|---------------|
| 1 | 2.50 | 1.92 | 6.25 | 3.70 | 2.55 | 70.0 |
| 2 | 1.32 | 1.19 | 1.76 | 1.42 | 0.34 | 9.45 |
| 3 | 2.08 | 1.25 | 4.34 | 1.56 | 2.78 | 76.5 |
| 4 | 1.72 | 1.39 | 2.96 | 1.93 | 1.03 | 28.2 |
| 5 | 0.85 | 0.61 | 0.72 | 0.38 | 0.34 | 9.3 |
| 6 | 1.25 | 0.64 | 1.56 | 0.41 | 1.15 | 32.6 |
| 7 | 1.07 | 0.67 | 1.16 | 0.45 | 0.70 | 19.2 |
| 8 | 0.58 | 0.35 | 0.34 | 0.13 | 0.21 | 5.8 |
| 9 | 0.42 | ---- | 0.19 | ---- | 0.19 | 5.2 |

Note: All shots were taken with a steel sphere
3/32" in diameter and wt. of 0.052 gm.

TABLE 3

1/8-Inch Plage Glass

| Shot No. | V_{impact} (km/sec) | V_{exit} (km/sec) | V_{in}^2 | V_{ex}^2 | $V_{\text{in}}^2 - V_{\text{ex}}^2$ | K.E. (joules) |
|-------------|---------------------------------|-------------------------------|-------------------|-------------------|-------------------------------------|---------------|
| 1 | 2.66 | 1.02 | 6.90 | 1.04 | 5.86 | 158.0 |
| 2 | 1.96 | 0.89 | 3.85 | 0.80 | 3.05 | 83.5 |
| 3 | 1.92 | 0.86 | 3.70 | 0.75 | 2.92 | 80.5 |
| 4 | 1.66 | 0.86 | 2.78 | 0.75 | 1.93 | 53.0 |
| 8 | 1.69 | 0.85 | 2.86 | 0.72 | 2.14 | 59.0 |
| 9 | 1.25 | 0.56 | 1.56 | 0.35 | 1.24 | 34.2 |
| 10 | 1.09 | 0.55 | 1.18 | 0.31 | 0.87 | 23.9 |
| 14 | 0.87 | ---- | 0.75 | ---- | 0.75 | 20.8 |
| 15 | 0.87 | 0.54 | 0.75 | 0.29 | 0.46 | 12.8 |
| 16 | 0.66 | 0.55 | 0.44 | 0.31 | 0.135 | 37.0 |
| 18 | 0.70 | ---- | 0.48 | ---- | 0.48 | 13.3 |
| 19 | 0.86 | 0.47 | 0.74 | 0.23 | 0.52 | 14.2 |
| 20 | 1.56 | 0.87 | 2.24 | 0.75 | 1.50 | 41.0 |
| 21 | 1.47 | 1.39 | 2.15 | 0.80 | 1.35 | 37.1 |
| 22 | 2.00 | 1.11 | 4.00 | 1.24 | 3.76 | 100.3 |

Note: All shots were taken with a steel sphere $3/32$ " in diameter and wt. of 0.052 gm.

TABLE 4
1/4-Inch Plate Glass

| Shot No. | V_{impact} (km/sec) | V_{exit} (km/sec) | V_{in}^2 | V_{ex}^2 | $V_{\text{in}}^2 - V_{\text{ex}}^2$ | K.E. (joules) |
|-------------|---------------------------------|-------------------------------|-------------------|-------------------|-------------------------------------|---------------|
| 1 | 1.85 | 1.51 | 3.43 | 2.30 | 1.13 | 31.0 |
| 2 | 1.85 | 1.66 | 3.43 | 2.75 | 1.68 | 44.0 |
| 3 | 1.92 | 1.47 | 3.70 | 2.15 | 1.55 | 42.5 |
| 15 | 1.47 | 1.09 | 2.15 | 1.18 | 0.97 | 26.8 |
| 18 | 0.78 | ---- | 0.57 | ---- | 0.57 | 15.7 |
| 19 | 0.58 | ---- | 0.33 | ---- | 0.30 | 9.1 |
| 20 | 1.66 | 0.73 | 2.76 | 0.54 | 2.22 | 61.0 |
| 21 | 2.50 | 0.96 | 6.25 | 0.92 | 3.98 | 100.9 |
| 22 | 1.66 | 0.62 | 2.76 | 0.39 | 1.77 | 48.6 |
| 23 | 1.61 | 0.89 | 2.60 | 0.80 | 1.34 | 36.8 |
| 24 | 1.92 | 0.74 | 3.70 | 0.54 | 2.26 | 62.0 |

Note: Shots were taken with a 3/32" diameter steel sphere of wt. 0.052 gm., except for shots 20 to 24, which were taken with a 1/16" diameter tungsten sphere of wt. 0.070 gr.

TABLE 5

1/2-Inch Plate Glass

| <u>Shot No.</u> | <u>V_{impact} (km/sec)</u> | <u>V_{exit} (km/sec)</u> | <u>V_{in}²</u> | <u>V_{ex}²</u> | <u>V_{in}² - V_{ex}²</u> | <u>K.E. (joules)</u> |
|---------------------|--|--------------------------------------|-----------------------------------|-----------------------------------|--|----------------------|
| 1 | 2.27 | ---- | 5.15 | ---- | 5.15 | 106.0 |
| 2 | 2.38 | ---- | 5.66 | ---- | 5.66 | 117.0 |
| 3 | 2.27 | ---- | 5.15 | ---- | 5.15 | 106.0 |
| 4 | Test | | | | | |
| 5 | 2.00 | ---- | 4.00 | ---- | 4.00 | 82.0 |
| 6 | 2.08 | ---- | 4.34 | ---- | 4.34 | 89.0 |
| 7 | 1.70 | ---- | 2.90 | ---- | 2.90 | 62.0 |

Note: Shot No. 2 just perforated the glass. All recorded shots were taken with 1/16" tungsten sphere of wt. 0.070 gm.

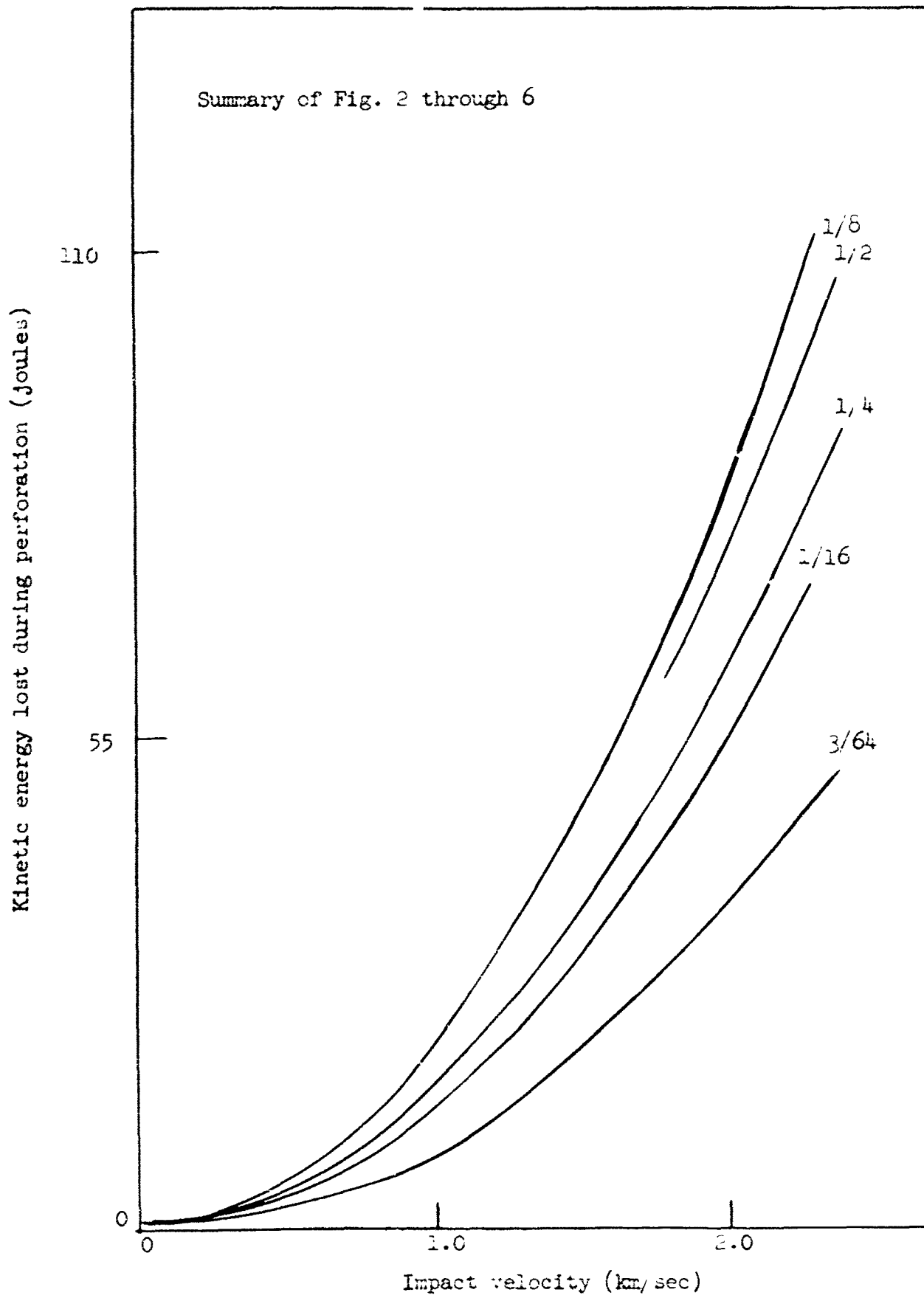


Fig. 7

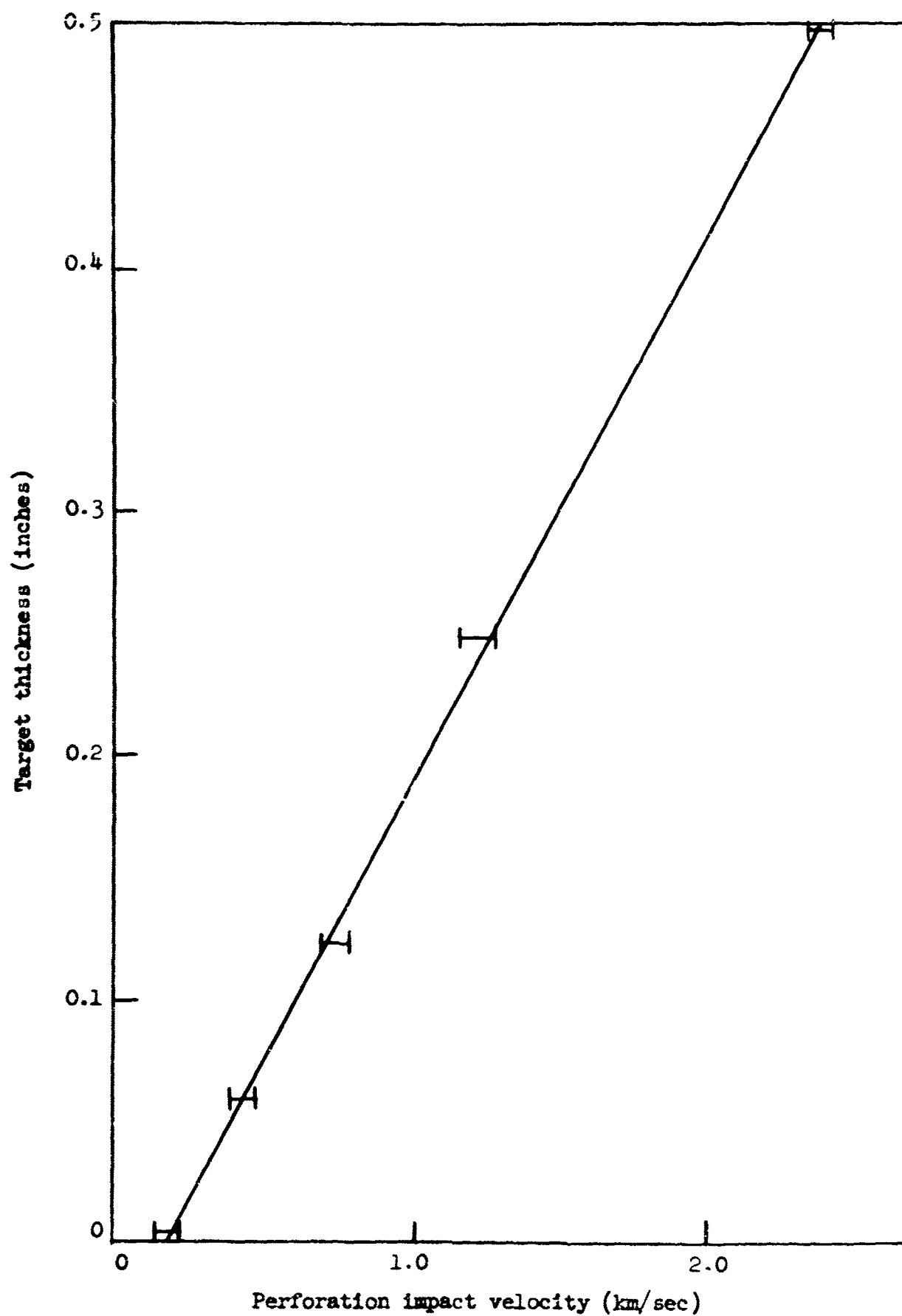


Fig. 8

lost as a function of impact velocity for the tungsten was essentially the same as for the steel sphere; therefore, the deformation as a function of impact velocity was not determined. The pictures on page 24 illustrate the effect of impact velocity and target thickness upon steel pellet deformation.

Since glass fracture usually occurs perpendicular to the tensile stress, observation of the fracture pattern will reveal the pattern of the most severe tensile stress. Examination of the targets revealed that the fracture in glass could be attributed to several phenomena resulting from the transfer of energy from the pellets to the target. These phenomena were: (1) The creation of modes of vibration peculiar to thin rectangular plates and membranes,¹² (2) the reflection of a compression wave from a boundary,¹³ (3) the radial distribution of cracks around the impact center,¹⁴ (4) the spallation of the rear surface of the target,¹⁵ and (5) the large fracture concentration, at various velocities of impact, occurring between the front and rear surfaces.¹⁶

It seemed that regardless of the impact velocity or energy of the pellet, the fracture due to the second and third modes of vibration existed in the glass target.¹⁷ Since more complicated fracture patterns occurred at the higher impact energies, due to the increased importance

12. Timoshenko, "Vibration Problems in Engineering," Van Nostrand Co., Inc., New York (1928).

13. Op. cit., Stanworth.

14. Op. cit., Kolsky.

15. Op. cit., Stanworth.

16. Op. cit., Charles.

17. Op. cit., Timoshenko.



Fig. 9. Modes of vibration of thin rectangular plates.

of other phenomena, observation of the fracture due to the lower modes of vibration was most emphatically demonstrated near the perforation velocities for the glass. This is illustrated by the mirror photographs on pages 25 and 26. The impact surface of the target is on the left side.

Tension fracture at an edge resulting from reflection of the compression wave from a boundary was also well illustrated when the velocity of impact is low but somewhat above that required for perforation, as shown by the photographs on pages 27 and 28.

It was found that when the ratio of the impact velocity to the velocity of sound in glass was $1/2$ or larger, the number of radial fractures occurring near the impact center greatly increased in number and diminished in size and the glass had the appearance of a fine powder near to the impact center. Also in this velocity region, especially for the thicker targets, $1/4$ and $1/2$ inch, it was observed that a large stress concentration occurred between the surfaces of the glass, resulting in a disc-shaped hole within the glass. These phenomena are illustrated by the photographs on page 29 and by Figure 10 on page 30.



Fig. B. Steel pellets shot into 1/8-inch plate glass at velocities of 2.5, 1.8, 1.2, 0.6, and 0.0 km/sec., as read from left to right.



Fig. C. Steel pellets shot into 3/6r-inch plate glass at velocities of 2.5, 1.8, 1.2, 0.6, and 0.0 km/sec., as read from left to right.

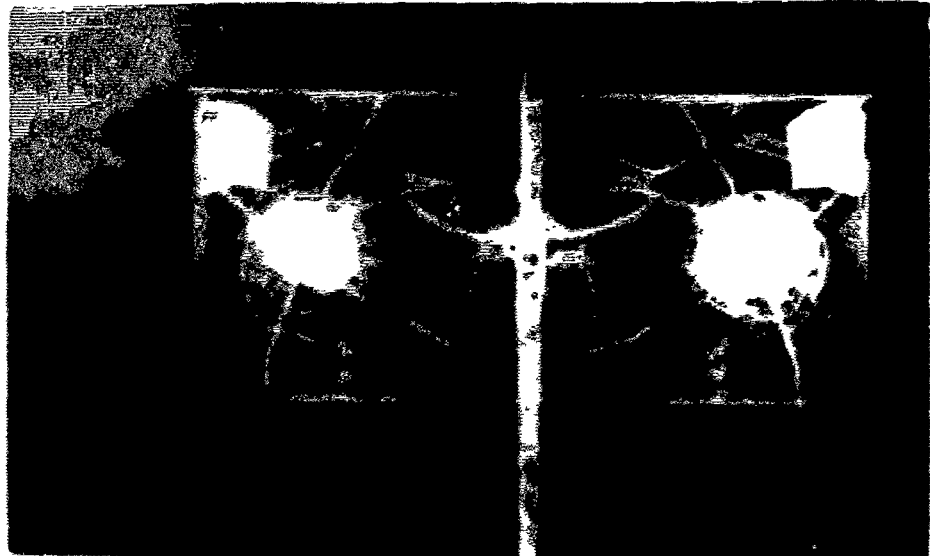


Fig. D. 1/4-inch plate $V_{\text{impact}} = 0.78 \text{ km/sec.}$



Fig. E. 1/8-inch plate $V_{\text{impact}} = 0.70 \text{ km/sec.}$

ILLUSTRATIONS OF LOWER MODES OF VIBRATION FRACTURE



Fig. F. 1/16-inch plate $V_{\text{impact}} = 0.42 \text{ km/sec.}$

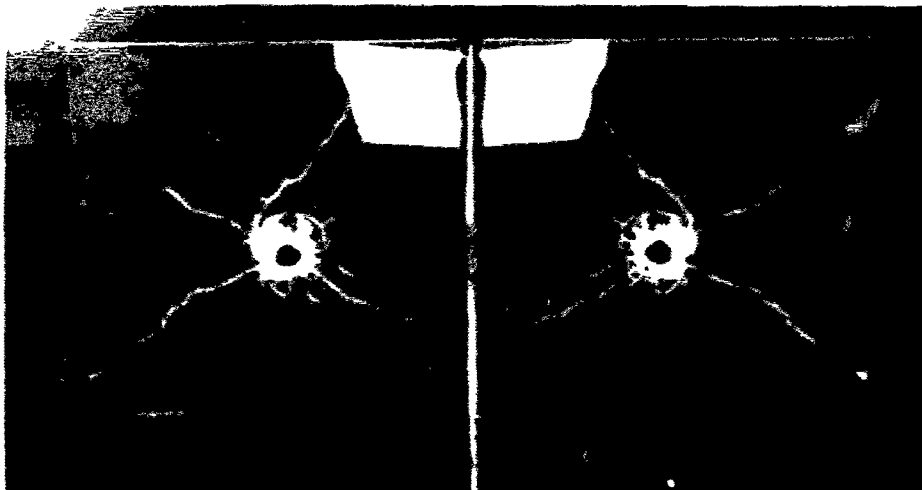


Fig. G. 3/64-inch plate $V_{\text{impact}} = 0.07 \text{ km/sec.}$

ILLUSTRATIONS OF LOWER MODES OF VIBRATION FRACTURE

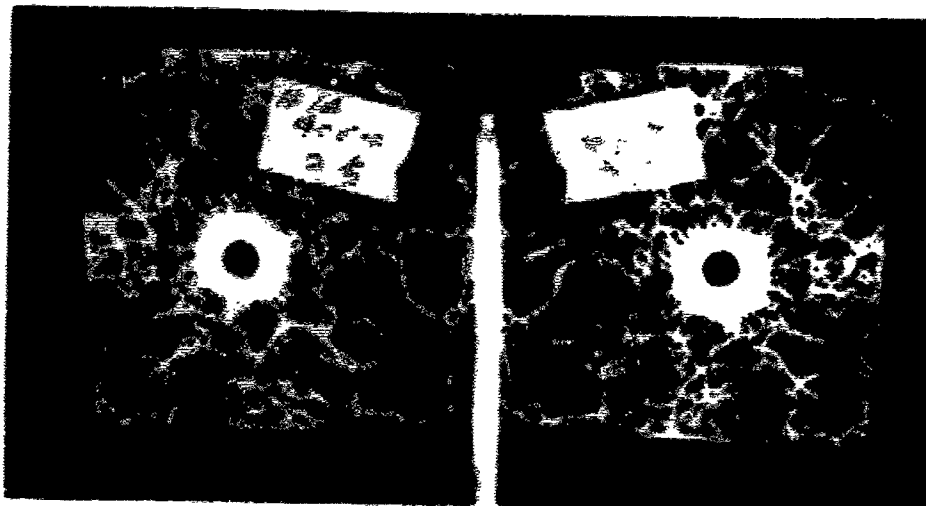


Fig. H. 1/8-inch plate $V_{\text{impact}} = 0.87$ km/sec.

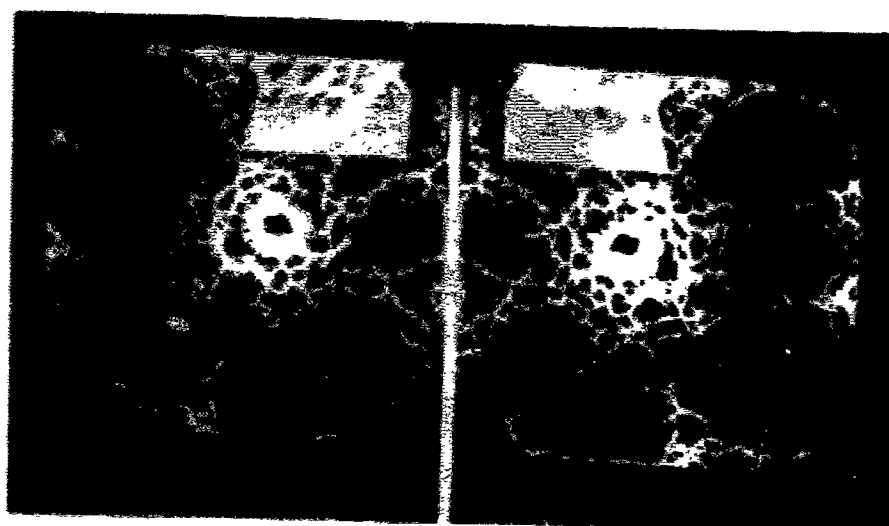


Fig. I. 1/16-inch plate $V_{\text{impact}} = 1.07$ km/sec.

ILLUSTRATIONS OF EDGE TENSION FRACTURE

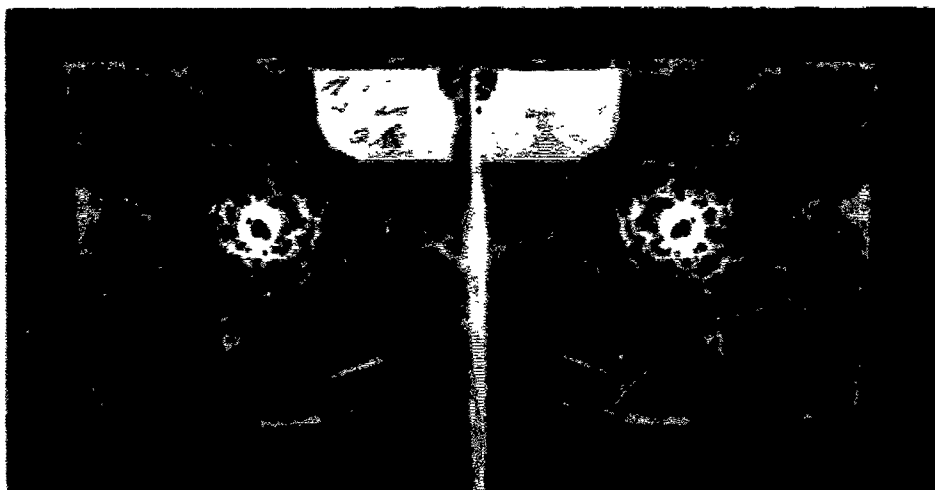


Fig. K. $3/64$ -inch plate $V_{\text{impact}} = 1.02 \text{ km/sec.}$

ILLUSTRATION OF EDGE TENSION FRACTURE

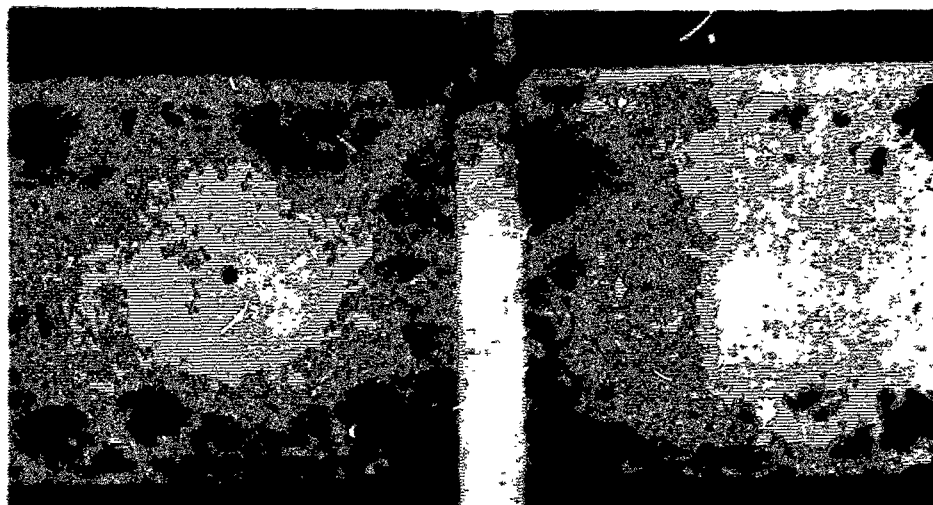


Fig. L. 1/2-inch plate $V_{\text{impact}} = 2.27$ km/sec.

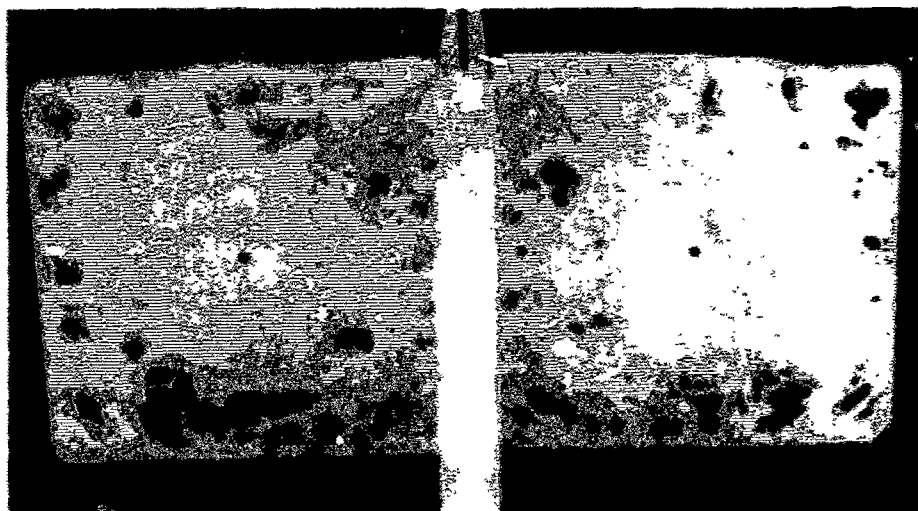


Fig. M. 1/2-inch plate $V_{\text{impact}} = 2.38$ km/sec.

ILLUSTRATION OF INTERNAL STRESS CONCENTRATION

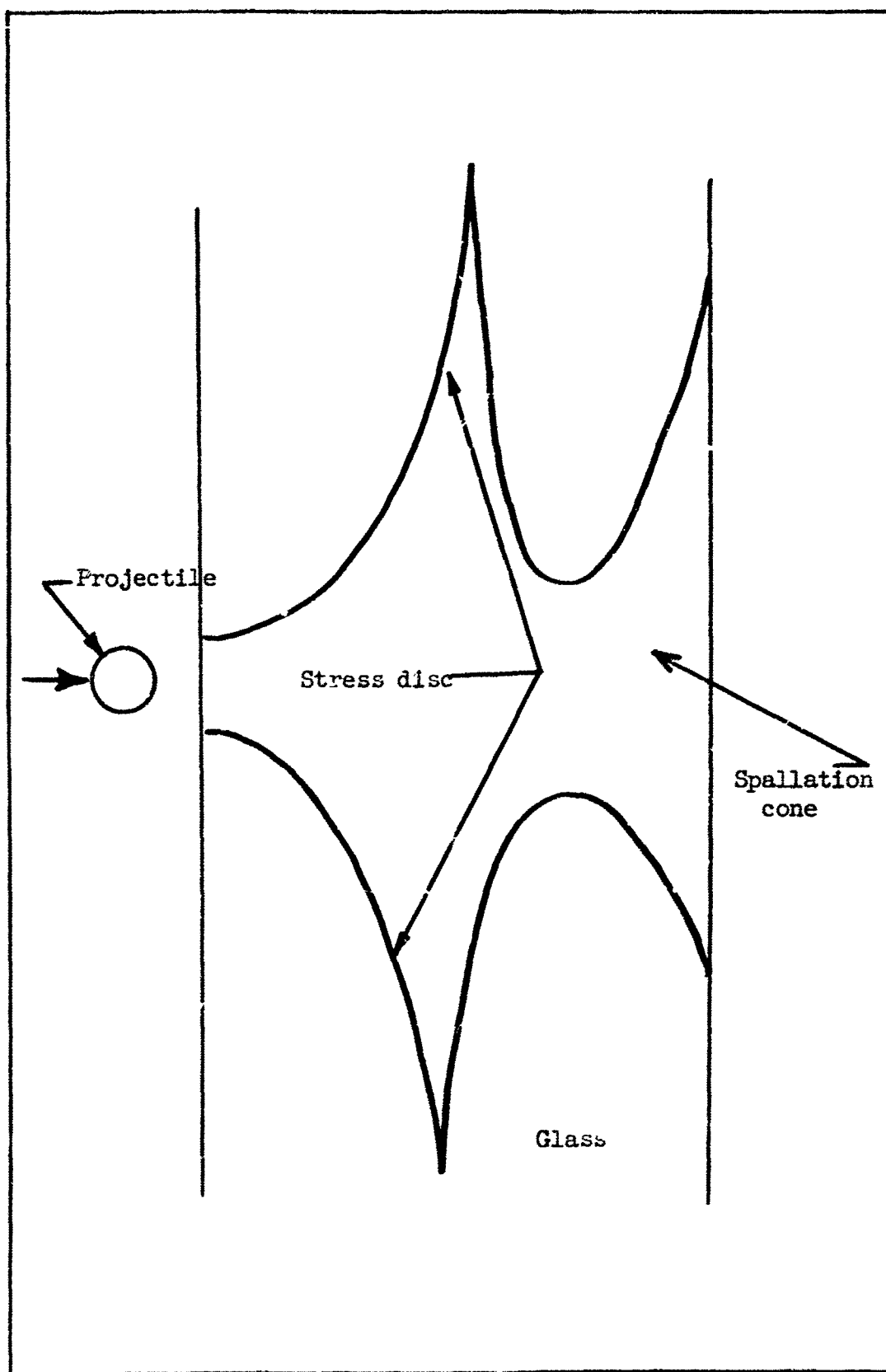


Fig. 10. Illustration of stress disc formed by internal stress concentration.

CONCLUSIONS

The energy required for perforation as a function of pellet impact velocity was found to approximate a straight line relationship. It was found that the energy the pellet lost during perforation as a function of impact velocity could be approximated by a parabolic relationship. It was also found that the calculated parabola for the 1/8-inch glass indicated a greater energy loss than the 1/4- and 1/2-inch glass for any impact velocity. The amount of energy required for deformation of the pellet and the relationship between target thickness and energy loss during perforation could be calculated and thereby eliminate some of the uncertainty in the evaluation of energy distribution, but until further, more refined measurements are made, the quantitative influence of resonant vibration, spallation and other methods of fracture upon the energy loss cannot be determined.

APPENDIX 1

TABLE 1

3/64-Inch Plate Glass

| <u>Shot No.</u> | <u>Load Type</u> | <u>Load Amount (cm³)</u> | <u>Δ Striking Time (μsec.)</u> | <u>Δ Exit Time (μsec.)</u> |
|---------------------|----------------------|---|--|------------------------------------|
| 1 | 2400 | 3V | 230 | 280 |
| 2 | 2400 | 3V | 220 | 275 |
| 3 | 2400 | 2.5V | 300 | 330 |
| 4 | 2400 | 2.5V | 280 | 340 |
| 5 | 2400 | 3 | 285 | 345 |
| 6 | 2400 | 3 | 350 | 375 |
| 7 | 2400 | 2 | 255 | 385 |
| 8 | 2400 | 2 | 345 | 370 |
| 9 | 4064 | | 360 | 480 |
| 10 | 4064 | 3 | 380 | 450 |
| 13 | 4064 | 1.5 | 490 | --- |
| 14 | 4064 | 1.5 | 460 | --- |
| 16 | 2400 | 3V | 260 | 320 |
| 17 | 2400 | 3V | 320 | 360 |
| 18 | 2400 | 3V | 290 | 380 |
| 19 | 2400 | 3V | 215 | 265 |
| 20 | 2400 | 3 | 250 | 305 |
| 21 | 2400 | 3 | 351 | 370 |
| 22 | 2400 | 3 | 249 | 290 |

Note: 3V means that the volume of the charge was 3 cm³
and that the barrel was evacuated before firing.

TABLE 2

1/16-Inch Plate Glass

| <u>Shot No.</u> | <u>Load Type</u> | <u>Load Amount (cm³)</u> | <u>Δ Striking Time (μsec.)</u> | <u>Δ Exit Time (μsec.)</u> |
|---------------------|----------------------|---|--|------------------------------------|
| 1 | 2400 | 3V | 270 | 580 |
| 2 | 2400 | 3 | 2400 | 400 |
| 3 | 2400 | 3V | 200 | 260 |
| 4 | 2400 | 2 | 290 | 360 |
| 5 | 2400 | 1.5 | 590 | 810 |
| 6 | 2400 | 1.5 | 400 | 780 |
| 7 | 4064 | 2.5 | 465 | 740 |
| 8 | 4064 | 1.5 | 850 | 1400 |
| 9 | 4064 | 1.5 | 1150 | --- |

TABLE 3

1/8-Inch Plate Glass

| <u>Shot No.</u> | <u>Load Type</u> | <u>Load Amount (cm³)</u> | <u>Δ Striking Time (μsec.)</u> | <u>Δ Exit Time (μsec.)</u> |
|---------------------|----------------------|---|--|------------------------------------|
| 1 | 2400 | 3V | 190 | 490 |
| 2 | 2400 | 3V | 255 | 560 |
| 3 | 2400 | 2.5V | 260 | 580 |
| 4 | 2400 | 2.5V | 300 | 580 |
| 5 | 2400 | 3 | 280 | 450 |
| 6 | 2400 | 3 | --- | --- |
| 7 | 2400 | 2.5 | 295 | --- |
| 8 | 2400 | 2.5 | --- | 590 |
| 9 | 2400 | 2 | 400 | 890 |
| 10 | 2400 | 2 | 460 | 900 |
| 11 | 4064 | 2.5 | 480 | --- |
| 15 | 4064 | 2 | 574 | 925 |
| 16 | 4064 | 2 | 750 | 900 |
| 17 | 4064 | 1.5 | 720 | --- |
| 19 | 2400 | 1.5 | 580 | 1040 |
| 20 | 2400 | 3V | 320 | 575 |
| 21 | 2400 | 3V | 240 | 561 |
| 22 | 2400 | 3V | 250 | 450 |

TABLE 4

1/4-Inch Plate Glass

| <u>Shot No.</u> | <u>Load Type</u> | <u>Load Amount (cm³)</u> | <u>Δ Striking Time (μsec.)</u> | <u>Δ Exit Time (μsec.)</u> |
|-----------------|------------------|-------------------------------------|--------------------------------|----------------------------|
| 1 | 4064 | 3 | ng | ng |
| 2 | 4064 | | 360 | ng |
| 3 | 4064 | 2.5 | 270 | 330 |
| 15 | 2400 | 3 | 340 | 460 |
| 18 | 4064 | 1.5 | 870 | --- |
| 19 | 4064 | 1.5 | 660 | --- |
| 4 | 2400 | 2.5 | 270 | 360 |
| 5 | 2400 | 2.5 | 260 | 340 |
| 6 | 4064 | 2 | 495 | --- |
| 7 | 4064 | 2 | 550 | --- |
| 8 | 4064 | 2 | 560 | --- |

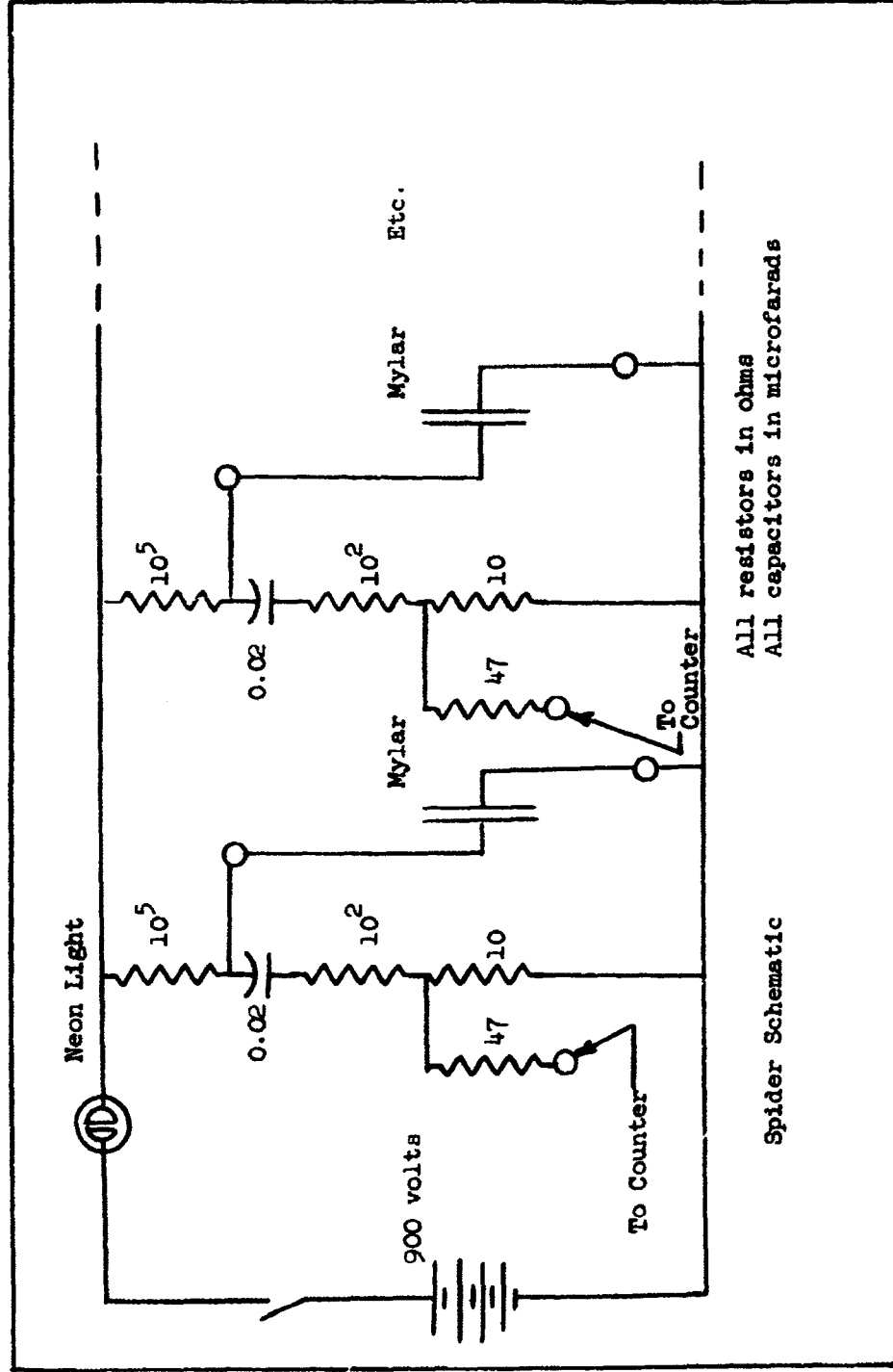
TABLE 5

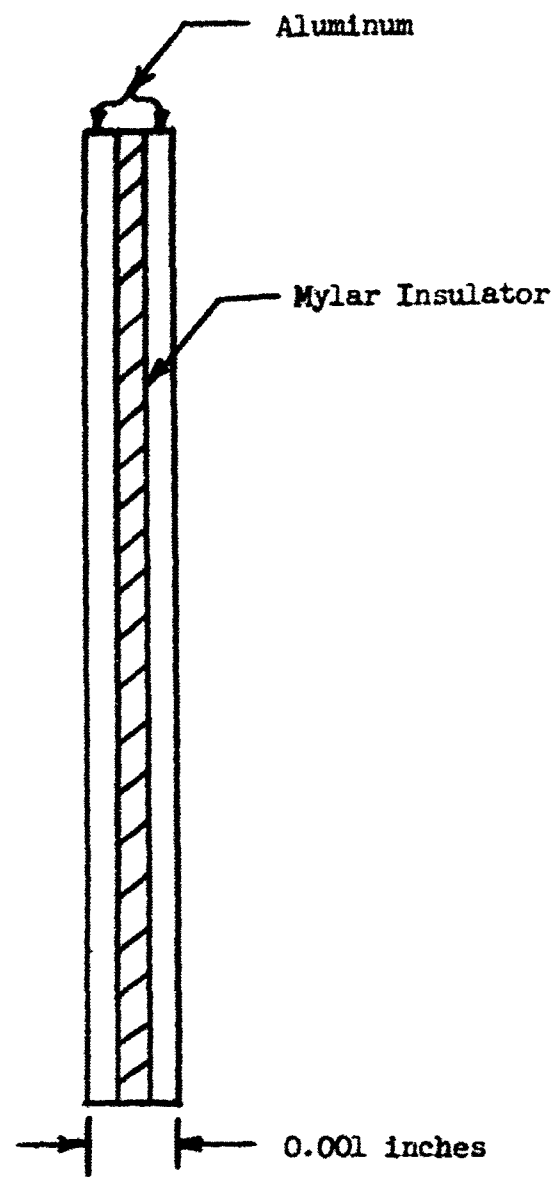
1/2-Inch Plate Glass

| <u>Shot No.</u> | <u>Load Type</u> | <u>Load Amount (cm³)</u> | <u>Δ Striking Time (μsec.)</u> | <u>Δ Exit Time (μsec.)</u> |
|-----------------|------------------|-------------------------------------|--------------------------------|----------------------------|
| 1 | 2400 | 3V | 220 | --- |
| 2 | 2400 | 3V | 210 | --- |
| 3 | 2400 | 3V | 220 | -- |
| 4 | 2400 | 2.5V | 250 | --- |
| 6 | 2400 | 2.5V | 240 | --- |
| 7 | 2400 | 3 | 294 | --- |

Note: Shot No. 2 just penetrated the glass.
All shots were made with tungsten.

APPENDIX 2





MYLAR FOIL

* Mylar foil is made by the National Metalizing Corp.